CONF

CONF-810831--29

SWELLING, MICROSTRUCTURAL DEVELOPMENT AND HELIUM EFFECTS IN TYPE 316 STAINLESS STEEL IRRADIATED IN HFIR AND EBR-II*

P. J. Maziasz and M. L. Grossbeck
Metals and Ceramics Division, Oak Ridge National Laboratory
Oak Ridge, Tennessee 37830

MASTER

This work examines the swelling and microstructural development of a single heat of 20%-cold-worked type 316 stainless steel irradiated to produce displacement damage and a high, continuous helium generation rate, in the High Flux Isotope Reactor (HFIR). Similar irradiation of the same heat of steel in the Experimental Breeder Reactor (EBR)-II is used as a base line for comparing displacement damage accompanying a very low continuous helium generation rate. At temperatures above and below the void swelling regime (~350 to 625°C) swelling is greater in HFIR than in EBR-II. In the temperature range of 350 to 625°C, cavity formation, precipitation and dislocation recovery are both enhanced and accelerated in HFIR, often causing swelling at lower dose than in EBR-II. In HFIR, however, cavities appear to be bubbles rather than voids. They are about 10 times smaller and 20 to 50 times more numerous than voids in EBR-II. Thus, the swelling becomes greater in EBR-II than in HFIR for 20%-CW 316 in the void swelling temperature ranges as fluence increases. Such differences in swelling and microstructural behavior must be understood in order to anticipate the behavior of materials during fusion irradiation.

INTRODUCTION

Helium effects were first studied in conjunction with the behavior of rare gases like xenon and krypton in uranium fuels [1,2], but then became directly important for bubble swelling and embrittlement of fuel cladding and core components for breeder reactors. Helium bubble formation has long been thought to be critical for void formation in stainless steels [3,4], and current work confirms and expands its important effects on general cavity formation [5]. Irradiated stainless steels usually have faulted loop formation, dislocation recovery, and precipitation of various phases occurring together with the void swelling phenomena. Determining the relationships between processes or the dominant process can be very difficult. Bubble swelling is a separate phenomenon that can occur when enough helium is present and can cause swelling under thermal aging with no irradiation. Bubbles can become voids and voids can be annealed back to bubbles, and the controlling mechanisms for growth of either are not necessarily the same. Understanding the effects of increased helium generation during irradiation is important for anticipating fusion response, particularly since much of our conventional wisdom on radiation effects comes from the fast breeder reactor (FBR) program where helium effects can be quite obscure.

This work is intended to highlight and expand upon recent work on swelling and microstructural development of type 316 stainless steel (DO-heat) irradiated in HFIR and in EBR-II [6–9]. A comprehensive review of helium and irradiation effects, elsewhere in these proceedings [10] for the purpose of fission-fusion properties correlation also includes this work. New information in this work includes determination of swelling rates for 20%-cold-worked (CW) 316 irradiated in HFIR and a detailed comparison of swelling and microstructural development at several fluences in EBR-II and HFIR. Irradiation and transmission electron microscopy (TEM) experimental details can be found elsewhere [6–9].

RESULTS

A Swelling in HFIR

Figures 1 and 2 show the temperature and fluence dependence of swelling for 20%-cold-worked (CW) 316 irradiated in HFIR below about 625°C. Together these figures illustrate the important points about the swelling behavior in HFIR. In Fig. 1, all cavity volume fraction (CVF) swelling values at 600°C and below are less than ~3.5% for fluences up to 60 dpa. Together, the high and low fluence curves show highest swelling to occur at the lower and upper temperature ends of the range, with flat or minimum swelling behavior in the vicinity of 400 to 575°C. Previous work indicates that at low fluence, the apparent low temperature swelling maxima appears to be due to void-like cavities with no concurrent precipitation effects [9]. Precipitation of phases, primarily eta (η) and Laves, occurs above 300°C, with maximum precipitation coinciding with the minima in the swelling curves. With the exception of large 100-nm-dia cavities, that may be voids, attached to eta phase particles after irradiation at 380°C to 49 dpa, all other cavities observed above 300°C appear, on the basis of size, location, and particularly gas balance calculations, to be equilibrium bubbles [9]. The sharp upturn in swelling at high fluence above 550°C coincides with both recrystallization of the cold-worked structure together with grain growth and with the onset of large cavity formation at the grain boundaries. At low

*Research sponsored by the Office of Fusion Energy, U.S. Department of Energy, under Contract No. W-7405-eng-26 with the Union Carbide Corporation.

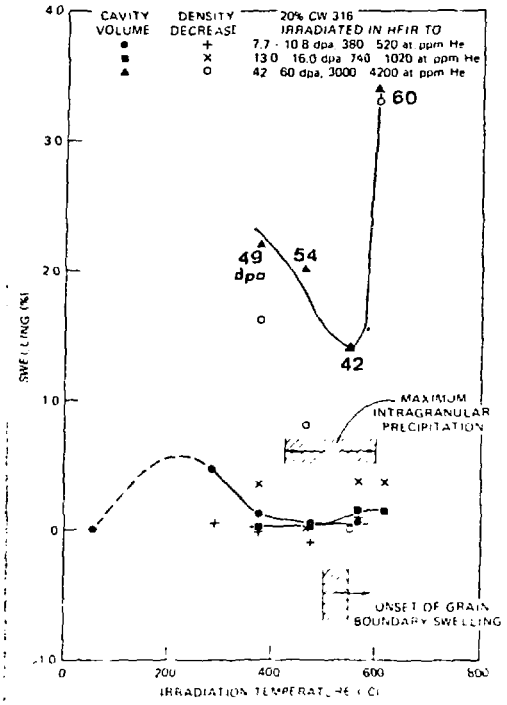

Fig. 1. Temperature dependence of swelling for 20%-cold-worked (DO-heat) 316 irradiated in HFIR. The shaded regions indicate the temperature range over which the stated microstructural effects occur.

fluence, the immersion density changes are quite close in value and parallel in trend to CVF data. At high fluence, the immersion density changes are parallel to but considerably lower (up to 550°C) than the CVF swelling values. These differences, in part, reflect the densification due to considerable precipitation of eta and Laves occurring at these temperatures.

Figure 2 shows the fluence dependence of the same data pictured in Fig. 1. The similar swelling rates for temperatures between 375 and 620°C in Fig. 2 are consistent with the flat or minimum regions shown in Fig. 1. The swelling values that connect high and low fluence data measurements are calculated from curves describing the fluence dependence of the microstructural parameters of average cavity diameter and cavity concentration [7]. Despite considerable variation of the microstructual parameters with temperature and fluence, the swelling curves in Fig. 2 are quite parallel and indicate steady state type swelling behavior above about 30 dpa.

B. Comparison of Swelling and Microstructural Development in HFIR and EBR-II

This section compares the same heat of 20% CW 316 (DO-heat) irradiated in HFIR at 460–475°C and in EBR-II at 500–525°C. Temperatures are

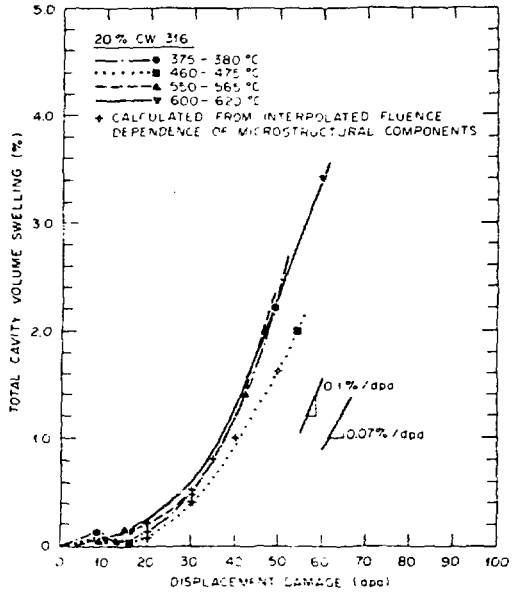

Fig. 2. Fluence dependence of swelling for 20%-cold-worked 316 irradiated in HFIR.

calculated in both HFIR and EBR-II, and the same temperatures are not available in both reactors. The above comparison was chosen because all available temperature data in HFIR indicates that the actual irradiation temperatures are probably 50 to 100°C higher than the calculated irradiation temperatures [6,7]. Analysis is still in progress, but the temperatures are certainly no lower than calculated. High fluence EBR-II data for this comparison come from the work of Brager and Garner [11].

The fluence dependence of CVF swelling in the two reactors is shown in Fig. 3. This figure shows early CVF swelling in HFIR greater than that in EBR-II below about 30 dpa. However, at higher fluence the EBR-II-irradiated material exhibits rapid and steady state void swelling that is both greater in magnitude and in rate than the bubble swelling found in HFIR. Because the data below about 60 dpa fall close together, we must examine the microstructures that go with these data points to justify the curves that indicate different swelling rates.

Figures 4–6 compare the microstructures at several fluences for EBR-II and HFIR irradiation of 20%-CW DO-heat 316 and Fig. 7 summarizes graphically some of these microstructural parameters important for understanding the differences shown in Fig. 3. The microstructures shown in Fig. 4 indicate that cavity formation, precipitation of eta and Laves phases and dislocation recovery are much more rapid in HFIR compared to EBR-II-irradiated material at low fluence. There is some dislocation recovery, no cavity

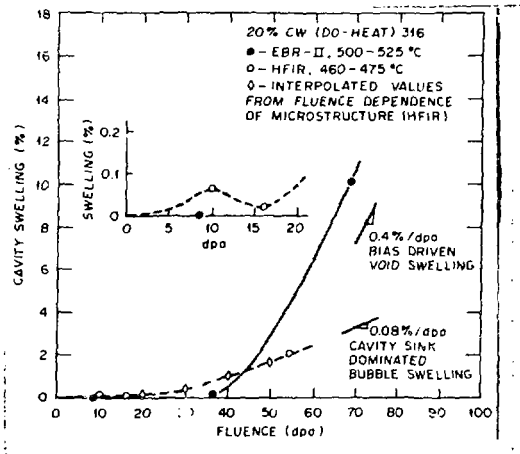

Fig. 3. Comparison of swelling as a function of fluence for 20%-cold-worked (DO-heat) 316 irradiated in HFIR and in EBR-II. Data at 69 dpa (EBR-II) is taken from Brager and Garner [11].

formation, and very little precipitation in EBR-II at 8.4 dpa. The fluence dependence of cavity sizes and cavity concentrations in HFIR and EBR-II at these conditions can be seen in Fig. 8. The cavities present in HFIR give the swelling observed in Fig. 3, whereas the low fluence EBR-II sample has no cavities — hence, no swelling. The dislocation density imaged in Fig. 4 show more recovery at lower fluence in HFIR than in EBR-II with both then remaining at a density of $1–2 \times 10^{14}$ m/m^3 at higher fluences. In both HFIR and EBR-II there is more recovery than will occur at similar temperatures during thermal aging. During thermal aging and HFIR irradiation, the dislocation recovery and precipitation phenomena are occurring together. During EBR-II irradiation, however, significant recovery occurs before significant precipitation begins. However, as fluence increases in EBR-II the amount of precipitation developed will approach that observed in HFIR, and both void and bubble formation will occur at 500–525°C.

The microstructures of Fig. 5 show development of a spatially heterogeneous void distribution after EBR-II irradiation at ~525°C to 36 dpa. Some regions have large voids [Fig. 5(a)], while other regions have none [Fig. 5(b)]. There is copious formation of eta and Laves phases uniformly in both regions, with a small amount of tau ($M_{23}C_6$) as well. X-ray EDS clearly indicates that both eta and Laves phase are rich in nickel and silicon at this fluence. Tau is found to be nickel and silicon poor, after irradiation, as it normally is after thermal aging. The voids appear to be forming in the regions that have the largest distance between the precipitate laden stacking fault bands. Some voids are attached to precipitate particles of eta and Laves, but many, including some of the largest, are free in the matrix. About one-fifth of the area observed appears like Fig. 5(a) (with about 0.1% local CVF swelling or less) and about four-fifths appear like Fig. 5(b) giving essentially no swelling, for an average of about 0.05% or less CVF swelling, as shown in Fig. 3. Figure 7(a) and (b) shows that the voids range in diameter from 20 to 140 nm with an average of about 70 nm with non-uniform concentrations ranging locally from $2–7 \times 10^{18}$ voids/m^3. The dislocation network continues to recover slowly with continued irradiation in EBR-II from 8.4 to 36 dpa, consistent with the increased swelling, but this appears to saturate from 36 to 69 dpa [11]. The most important information for discerning the effects of helium comes from high magnification examination of a typical no-void region in a kinematical diffracting condition, underfocused so that bubbles or cavities might appear bright, in Fig. 5(c). There are tiny cavities about 2–4 nm in diameter at a concentration $\sim 5–7 \times 10^{20}$ m^{-3}. These are most probably bubbles because they are located on matrix dislocations and at precipitate interfaces. They are the same size as obvious bubbles found at the grain boundaries [6]. The voids developing in regions like Fig. 5(a) are also located at precipitate interfaces and in the matrix. More data presented elsewhere also indicates that bubbles formed earlier at dislocations and precipitate interfaces are later developing into voids in EBR-II [6]. Brager and Garner have examined this same material reirradiated in EBR-II at ~510°C to

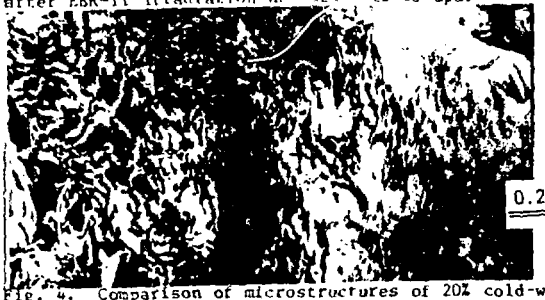

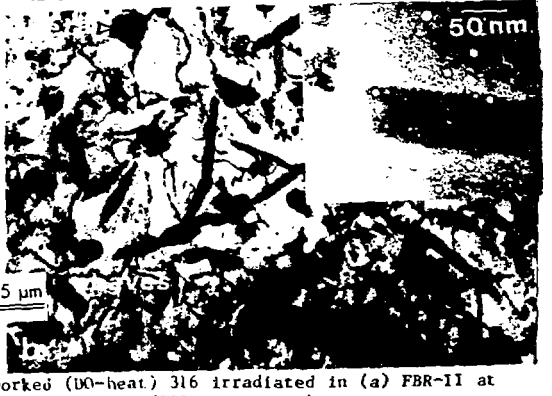

Fig. 4. Comparison of microstructures of 20% cold-worked (DO-heat) 316 irradiated in (a) FBR-II at 500°C to 8.4 dpa (~5 at. ppm He), and (b) HFIR at 475°C to 10 dpa (500 at. ppm He).

Fig. 5. Heterogeneous microstructural development in 20%-cold-worked (DO-heat) 316 irradiated in EBR-II at ~525°C to 36 dpa (~22 a . ppm He). (a) Typical void area, (b) typical void-free area, and (c) high magnification (kinematical, underfocused) to show tiny cavities (most probably bubbles) in both areas.

finally achieve 69 dpa [11]. The measured void CVF is shown in Fig. 3 for the EBR-II swelling curve and the microstructural statistics are included in Fig. 7(a) and (b). Swelling, as shown in Fig. 3, therefore, increases tremendously in EBR-II due primarily to increasing the population of voids, while somewhat increasing void size. It seems quite reasonable that the bubbles present at 36 dpa could transform to voids at high fluence if they grow according to a typical critical radius argument.

Figure 6 compares typical microstructures produced in HFIR after 54 dpa with a typical void containing region after 36 dpa in EBR-II. The microstructures in Fig. 6 along with the data in Fig. 7(a) emphasize the very large difference in size and concentration between voids (in EBR-II) and bubbles (in HFIR). It is this difference in size and concentration that causes the swelling and swelling rate differences shown in Fig. 3. Comparison of microstructures both in Fig. 6 (and in ref. [6]) shows that rather than one large void per precipitate particle as in EBR-II we find many smaller cavities along the precipitate interfaces that are the same size as in the matrix in HFIR. The size, concentration, and nature of the phases are quite similar in EBR-II and HFIR for these irradiations. The source of the different swelling rates appears to be the high cavity sink strength, both at precipitate interfaces and in the matrix. The high sink strength produced in HFIR does not allow large voids to form but rather encourages bubbles that then continue to grow as helium is being generated in HFIR. Therefore the curves and differences in Fig. 3 become quite reasonable when we consider the details of the microstructural evolution responsible for the total swelling behavior.

In conclusion, there is little about the microstructural development responsible for swelling that is the same for the two reactors. Two aspects of the HFIR swelling data are surprising compared to normal FBR swelling trends. The first is the nearly temperature independent

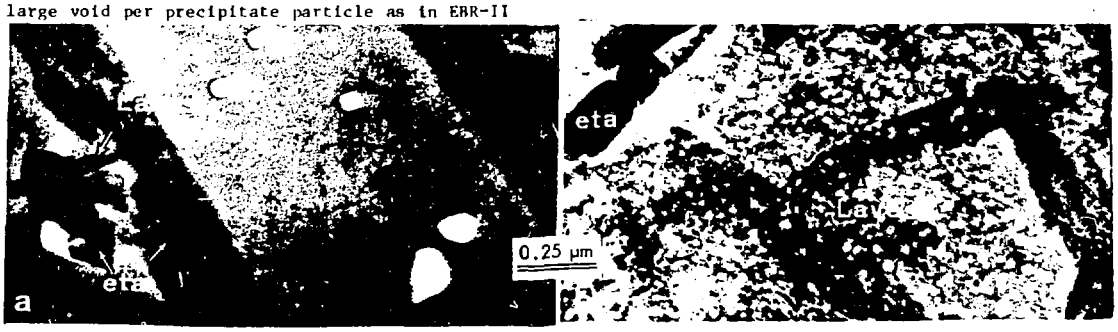

Fig. 6. Comparison of microstructures of 20%-cold-worked (DO-heat) 316 irradiated in (a) EBR-II at 525°C to 36 dpa (~22 at. ppm He) and (b) HFIR at 460°C to 54 dpa (~3600 at. ppm He.)

steady state swelling rate in HFIR compared to the considerable temperature dependence of swelling at similar irradiation conditions in EBR-II. The second is the low value of the steady state swelling rate of ~0.1%/dpa in HFIR because peak swelling rates at comparable irradiation conditions in EBR-II will peak at 0.4 to 0.5%/dpa. In general, low dislocation density and extensive precipitation, particularly of silicon and nickel rich phases, are considered quite favorable conditions for void development in EBR-II. Dislocation recovery and extensive precipitation of nickel and silicon rich phases occurs more rapidly and is complete at lower fluences in HFIR than in EBR-II for 20%-CW 316 in the 475 to 525°C temperature range. The cavities, however, are nucleated very early in HFIR, when the dislocation concentration is higher, at fluences of 1.5 to ~ dpa from 475 to 620°C. Therefore, the swelling behavior in HFIR is controlled by a high concentration of bubbles that are much smaller than voids found in EBR-II. These then become dominant sinks in the system to account for the slow swelling kinetics. The increased cavity concentration with increased helium generation rate during irradiation is an expected result. The reduced swelling rate resulting from the increased cavity sink strength is a consequence of this. Because the He/dpa ratio in HFIR becomes significantly greater than the fusion ratio after about 3 to 5 dpa [9], it is important to know when the microstructural features nucleated. Much work still remains for anticipating fusion microstructural development in order to correlate properties between fission and fusion environments [10]. The present work does make clear, however, that understanding helium effects is an important facet of this process.

REFERENCES

[1] Rimmer, D. E. and Cottrell, A. H., Phil. Mag. 2 (1957) 1345–53.

[2] Barnes, R. S. and Mazey, P. J. Proc. Roy. Soc. A275 (1963) 47– .

[3] Cawthorne, C. and Fulton, J. E., The Nature of Small Defect Clusters, ed., Makin, M. J., AERE Harwell Report AERE-R-5269, Vol. 2 (1966), pp. 446–60.

[4] Bloom, E. E. and Stiegler, J. O. J. Nucl. Mater. 36 (1970) 331–34.

[5] Farrell, K., Rad. Effects, 53 (1980) 175–94.

[6] Maziasz, P. J., ADIP Quart. Progr. Rept. Mar. 31, 1981, DOE/ER-0045/6, pp. 70–92.

[7] Maziasz, P. J. and Grossbeck, M. L., ibid., pp. 28–56.

[8] Maziasz, P. J. and Grossbeck, M. L., ADIP Quart. Progr. Rept. Dec. 31, 1980, DOE/ER-0045/5, pp. 43–69.

[9] Maziasz, P. J., Horak, J. A., and Cox, B. L., to be published in Proceedings of Symposium on Irradiation Effects on Phase Stability, (held in Pittsburgh, PA, Oct. 5–9, 1980).

[10] Odette, G. R., Maziasz, P. J., and Spitznagel, J. A., invited paper, elsewhere in this conference.

[11] Brager, H. R. and Garner, F. A., DAFS Quart. Progr. Rept. Oct.–Dec 1980, DOE/ER-0046/4.

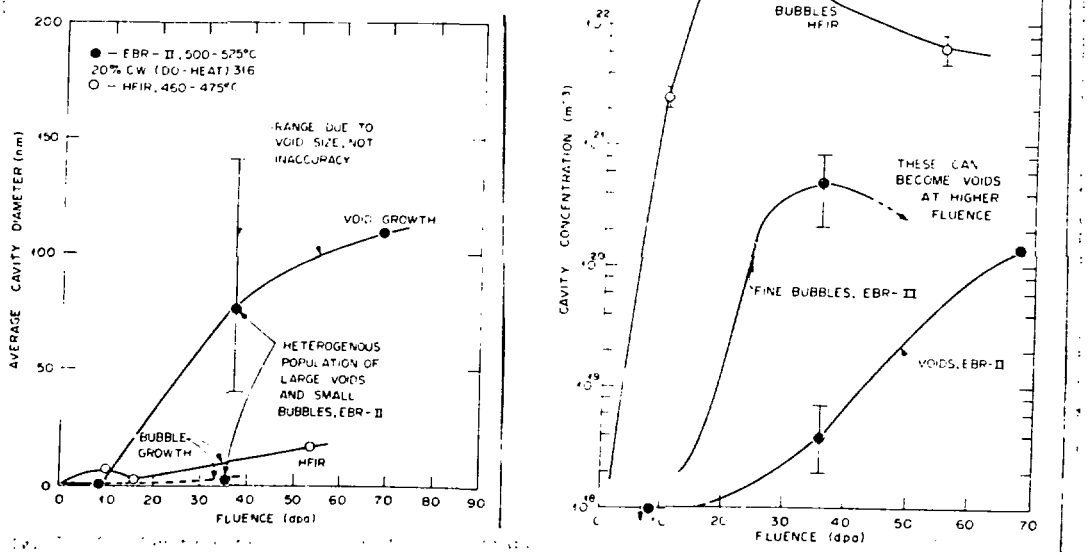

Fig. 7. (a) Cavity size and (b) cavity concentration as functions of fluence for 20%-cold-worked (DO-heat) 316 irradiated in EBR-II and HFIR. Data at 69 dpa (EBR-II) are taken from Brager and Garner [11].